ORGANIC
CHEMISTRY
FRONTIERS

Accepted Manuscript
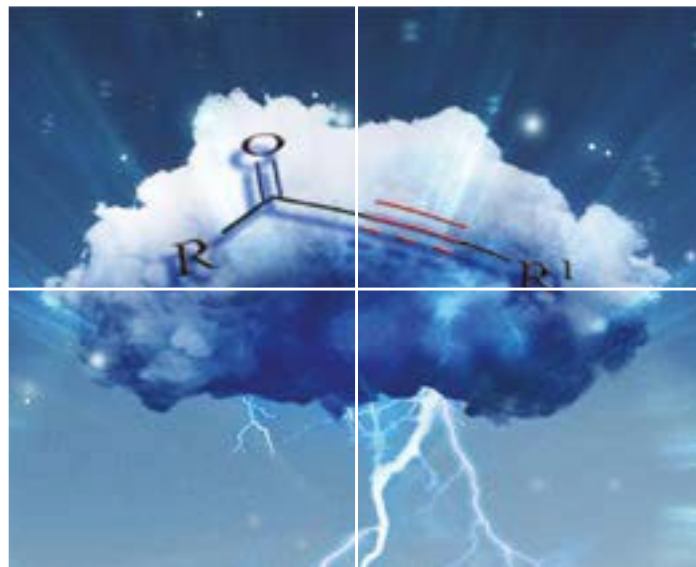
Volume 3 | Number 1 | January 2016

ORGANIC
CHEMISTRY
FRONTIERS

http://rsc.li/frontiers-organic

This is an Accepted Manuscript, which has been through the Royal Society of Chemistry peer review process and has been accepted for publication.

Accepted Manuscripts are published online shortly after acceptance, before technical editing, formatting and proof reading. Using this free service, authors can make their results available to the community, in citable form, before we publish the edited article. We will replace this Accepted Manuscript with the edited and formatted Advance Article as soon as it is available.

You can find more information about Accepted Manuscripts in the **author guidelines**.

Journal Name

ARTICLE

Supramolecularly Assisted Synthesis of Chiral Tripodal Imidazolium Compounds

Adriana Valls, Belén Altava,* M. Isabel Burguete, Jorge Escorihuela, Vicente Martí-Centelles, Santiago V. Luis*

Abstract A strong preference for the formation of tripodal systems over the related monotopic and ditopic compounds is observed for the reaction between tris(halomethyl)benzenes and imidazoles derived from aminoacids and containing an amide fragment. This preference allows the formation of the tripodal derivative as the very major product even when an equimolar mixture of the tris(halomethyl)benzene and the imidazole is reacted (1:1 ratio instead of the stoichimetric 1:3 ratio). The reactions were monitored using ^{1}H NMR spectroscopy and ESI mass spectrometry and kinetically characterized. Computational studies were also performed in order to rationalize the observed preference of the tri-substituted product. Results reveal the existence of well defined supramolecular interaction between the imidazolium groups and the reacting imidazoles that facilitate the formation of the multitopic systems once the first imidazolium group is formed. The analysis of the different structural components shows that the presence of the amide group from the aminoacid moiety is the key structural requirement for such supramolecular assistance to take place. The preorganization of the supramolecular intermediates formed through hydrogen bonding interactions involving amide-NH fragments in imidazoles and bromide anions in imidazolium groups, seems to be also present at the corresponding TSs, decreasing the associated energy barriers.

Introduction

In Nature, biomolecules are synthetized very efficiently, frequently triggered by external stimuli, through processes encompassing the appropriate supramolecular preorganization of the involved components. This is illustrated by enzymes displaying a high supramolecular preorganization.[1] Their catalytic activities depend on the presence in the active site of functional groups, often belonging to amino acids situated far away in the peptidic sequence, located at the right distances and orientations and facilitating the proper preorganization of the substrates for the corresponding reaction.[2,3]

A suitable preorganization of the substrates assisted by supramolecular interactions can also be important in abiotic systems, particularly for synthetizing macrocyclic structures.[4] In this case, the approaching of the two reactive ends is facilitated by the folding of the open-chain intermediate through hydrogen-bonding, conformational or configurational factors or by the use of templates.[5] For non-cyclic compounds, the formation of cyclic or chelate hydrogen bonds in close proximity of the target covalent bond can promote the desired reaction, facilitating the approach of the reactive elements.[6]

Thus, the development of structures able to control a hierarchically ordered synthesis is an important and challenging target.

Considerable efforts have been made in developing self-replicating systems.[7] In a model self-replicating system, the final molecule is able to selectively recognize the component fragments and preorganize them in the correct location as to promote the synthesis of a new identical molecule in a self-catalytic process.[8,9] If several interacting replicators are combined, then complex behaviours can occur as the network of cross and autocatalytic reactions increases in size.[10,11]

In this regard, the synthesis of polytopic receptors can benefit from a proper recognition by the monotopic intermediate of one of the components, favouring the synthesis of the ditopic system. The recognition of this component by the ditopic intermediate would favour the preparation of the tritopic compound and so on, eventually leading to polytopic systems even in the presence of a limited amount of the component being recognized. In this context, polytopic supramolecular imidazolium receptors are of current relevance taking into account their properties as receptors and transporters,[12,13] with tripodal imidazolium compounds providing flexible but selective 3D environments for anion recognition.[14] Thus, based on previous results of our group,[15] tripodal compounds displaying the general structure **I** (Figure 1) represented an interesting target, combining a well-defined 3D cavity with hydrogen bonding potential (amide and imidazolium moieties) with hydrophobic and aromatic regions playing essential roles in supramolecular recognition.[16] They integrate the

a. *Departamento de Química Inorgánica y Orgánica, Universitat Jaume I, Av. de Vicent Sos Baynat, s/n 12071, Castellón, Spain, E-mail: luiss@uji.es; altava@uji.es; Tel: +34 964728239; Fax: +34 964728214*

ARTICLE

supramolecular features of imidazolium compounds and those of amphiphilic pseudopeptides.[17] The synthetic approach is straightforward, involving the reaction of three equivalents of the corresponding imidazole with a tris(halomethyl)benzene. However, the accumulation of charge in the periphery of the aromatic fragments could hamper the introduction of the second and the third charged fragment. Rather surprisingly, preliminary experiments showed that even working with a defect of the imidazole (e.g. equimolar mixtures) the tripodal imidazolium compound was always preferentially obtained over the related mono- and ditopic molecules.
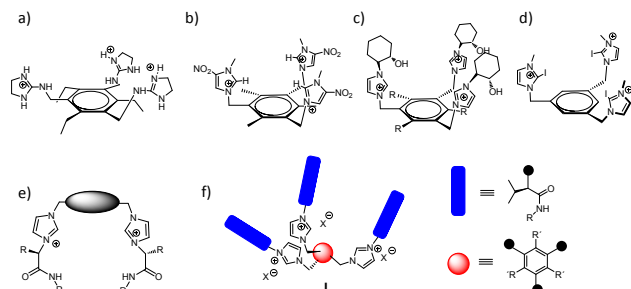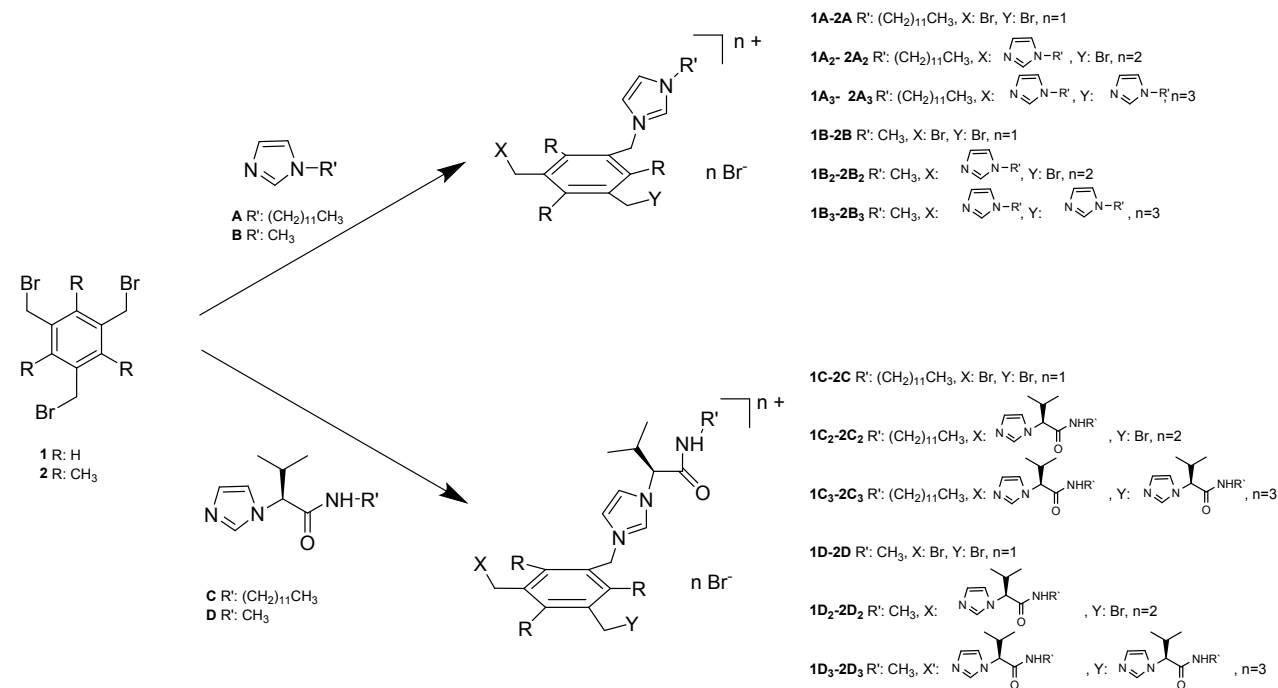

Figure 1 Polytopic supramolecular receptors based on imidazolium and related systems: a) citrate receptor, ref. 18b; b) halide recognition, ref. 14a; c) citrate and malate recognition, ref. 15a; d) anion recognition involving halogen-bonding

instead of hydrogen bonding, ref. 14f; e) transmembrane chloride transport and CSA for dicarboxylic acids, ref. 15b; f) tripodal receptors in this work.

In the light of these initial results, this process has been studied in detail to properly understand the specific supramolecular effects favouring the formation of the tripodal imidazolium species and the influence of the different structural elements. The combination of experimental results and computational studies has been essential for understanding the effects observed.

Results and Discussion

As shown in Figure 1, the general tripodal structure **I** contains three elements of diversity: the central aromatic core, the side chain of the amino acid used for the preparation of the imidazole ring and the length of the aliphatic chain attached to the amino acid moiety through an amide bond. The final synthetic step involves a [1+3] S_N2 process between a tris(halomethyl)benzene and an amino acid based imidazole (Scheme 1). Tris(halomethyl)benzenes are standard alkylating agents used in the synthesis of different tripodal receptors including imidazolium salts and pseudopeptic cages,[18,19] and the synthesis of the considered amino acid based imidazoles has been previously described.[20]

Scheme 1 Synthetic approach for the preparation of polytopic imidazolium compounds from the reaction between different imidazoles (**A**-**C**) and 1,3,5-tris(bromomethyl)benzene derivatives (**1**, **2**). The structure of each polyimidazolium compounds is denoted by three digits, the first one is a number related to the aromatic component (**1** or **2**), the second one indicates the imidazole used (**A**-**C**) and the third one, included as a subindex, defines the monoimidazolium (**NX$_1$**), bisimidazolium (**NX$_2$**) or tris(imidazolium) (**NX$_3$**) structure.

Initial experiments involving tris(bromomethyl)benzene **1** and the imidazole obtained from valine and containing a dodecyl aliphatic tail (**C**) (Scheme 1) revealed that the preparation of the corresponding tripodal trisimidazolium compound **1C$_3$** took place very efficiently. Even when a defect of imidazole was

used (equimolar **1**:**C** ratio) the tripodal derivative **1C$_3$** was the major species formed, while the monotopic (**1C**) and the ditopic (**1C$_2$**) imidazolium salts were only obtained as minoritary side products (**1C$_3$**: 73%, **1C$_2$**: 12% and **1C**: 5%).

Journal Name

ARTICLE

In order to analyse the generality of this process and its origin, the preparation of a family of imidazolium compounds, as shown in Scheme 1, was considered. To simplify this analysis, the amino acid component was fixed to be *L*-valine, while the alkyl chain attached to the amide nitrogen atom was either dodecyl (long aliphatic tail, imidazole **C**) or methyl (short aliphatic tail, imidazole **D**). Finally the alkylating agents selected were 1,3,5-tris(bromomethyl)benzene (**1**) and its 2,4,6-trimethyl derivative (**2**), previously used for the synthesis of tris(imidazolium) derivatives.[18,19] Commercially available N-dodecyl (**A**) and N-methyl (**B**) imidazoles were also studied as nucleophiles to provide proper comparison models lacking the amino acid based fragment.

¹H NMR and ESI-MS experiments. Initial kinetic experiments were carried out in CDCl₃ by ¹H NMR. To ensure that aggregation processes did not interfere, it was checked that these imidazoles do not aggregate in this solvent in the 1 to 60 mM range (ESI, Fig S1 for imidazoles **A** and **C**). Thus, the imidazole concentration was fixed in all experiments to *ca.* 15 mM in CDCl₃ and the reactions were carried out in an NMR tube. The temperature was maintained constant at 25ºC and dioxane (0.17 mM) was used as the internal standard. ¹H NMR spectra were obtained directly from these reaction tubes and the same reaction crudes were also analysed by ESI-MS. The reactions were monitored for up to *ca.* 700 h. Different tris(halomethyl)arene : imidazole molar ratios (*ca.* 1:3, 1:2 and 1:1) were assayed. Although some of the signals of interest could overlap at specific reaction times, ¹H NMR spectra allowed determining the concentration of the different species involved at the different time intervals.
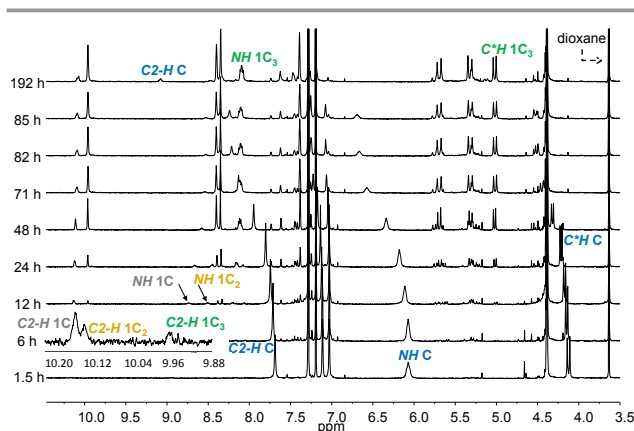

Figure 2 Partial ¹H NMR (400 MHz, CDCl₃) spectra obtained at different time intervals for the reaction of tris(bromomethyl)benzene **1** (13.8 mM) with imidazole **C** (13.8 mM) at 25ºC. The region around 10 ppm corresponding to the presence of C2-H signals of the imidazolium rings has been expanded for the spectrum after 6 h of reaction.

Figure 2 shows the ¹H NMR spectra for the process leading to **1C₃** when an equimolar mixture of the aromatic compound **1** and imidazole **C** was used. The signal corresponding to the C2-H proton of the imidazolium ring in **1C₃** was observed initially at ca. 10.03 ppm, while the signals for the mono- and di-substituted products appeared at 10.22 and 10.20 ppm respectively (see the expanded region after 6 h of reaction). These chemical shifts, and others used in this study, agreed

well with those obtained for the pure isolated **1C₃**, and for the model compounds **3** and **4** that had been prepared previously (Figure 3; ESI, Fig S2).[15a] The formation of **1C₃** could also be followed through the appearance of other characteristic signals like those for the amide NH and the proton at the stereogenic carbon atom (C*-H) initially at 8.22 and 5.08 ppm respectively. The signals originally at 7.78, 6.14 and 4.21 ppm, corresponding to the imidazole C2-H, amide NH and the C*-H of the starting imidazole **C** could be used to monitor its disappearance. Figure 4 gathers the kinetic profiles obtained for this reaction using these signals. Data presented in Figure 4 (top) for the equimolar mixture of **1** and **C** show clearly how the formation of the tripodal compound **1C₃** is significantly favoured over that of the mono- and di-substituted species **1C** and **1C₂**. After 77 h, the conversion of the starting imidazole **C** raised to *ca.* 65% with 46 % of these units incorporated into **1C₃**, 9 % of them into **1C₂** and only 9 % into **1C**. After this time, the concentration of **1C₃** continued increasing but not those of **1C₂** and **1C**. After 360 h, imidazole conversion reached *ca.* 90 %, with more than 72 % of the consumed imidazole groups incorporated into **1C₃**. The inset in Figure 4 reveals the existence of an apparent induction period for the formation of the bis- and tris-imidazolium derivatives **1C₂** and **1C₃** (*ca.* 3 and 4 h respectively), but not for **1C**, which has been often associated to processes involving autocatalytic steps or related processes.[7-10] Similar results were obtained when the **1:C** ratio was changed to 1:2.1 or 1:2.8 (ESI, Figure S3) with **1C₃** being always the major product obtained after *ca.* 24 h.
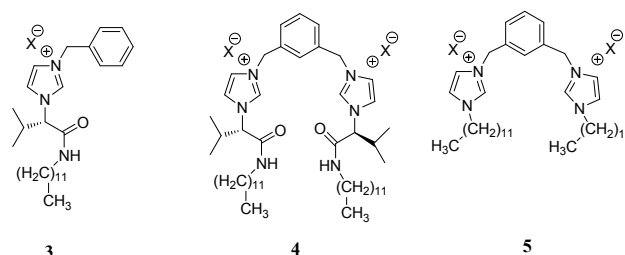
Figure 3. Model mono- and bis-imidazolium salts used for reference.
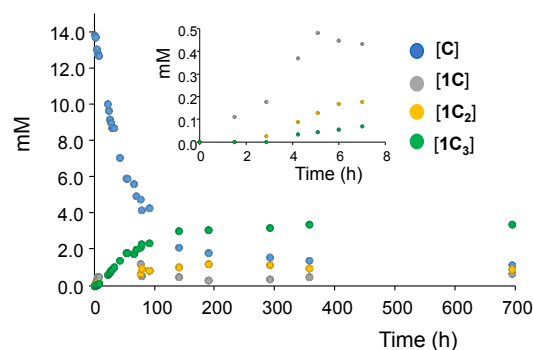
Figure 4. Variation with time of the concentration of the different species for an equimolar mixture (13.8 mM) of **1** and **C** as measured following the C2-H proton signals of the imidazolium compounds (green **1C₃**, yellow **1C₂**, grey **1C**) and those for the C*-H (blue) signal for **C**; the inset displays the formation of imidazolium species at initial times. Reaction carried out in CDCl₃ at 25ºC.

ESI-MS also allowed monitoring the reaction, identifying charged species associated to the starting imidazole building block **C** and to the tri-, di- and mono-imidazolium derivatives (**1C₃**, **1C₂** and **1C**). Thus, for the reaction between 1,3,5-tris(bromomethyl) benzene **1** and the imidazole **C** in an equimolar ratio, after 48 h, the ESI-MS in positive ion mode (Figure 5) contained a peak at m/z 612.4 for the monosubstituted compound [**1C**-Br]⁺ (100 % relative intensity) and a second minor peak at 434.6 (20 %) associated to the bisimidazolium compound [**1C₂**-2Br]²⁺. Species corresponding to the trisimidazolium product appeared at 374.6 and 602.0 associated to [**1C₃**-3Br]³⁺ (75 %) and [**1C₃**-2Br]²⁺ (80 %, this peak can also contain contributions from [**1C₂**-2Br+**C**]²⁺) and at 486.6 (10 %), 598.2 (20 %) and 710.2 (9 %) related to the **1C₃**:**C** clusters [**1C₃**-3Br+**C**]³⁺, [**1C₃**-3Br+2**C**]³⁺ and [**1C₃**-3Br+3**C**]³⁺. Moreover at 336.3 (50 %) and 671.8 (16 %) appeared peaks associated to [**C**+H]⁺ and [**C**+**C**+H]⁺ species from unreacted imidazole. After 697 h the peak at 612.4 for [**1C**-Br]⁺ decreased significantly (20 %) while the peak at 434.6 associated to [**1C₂**-2Br]²⁺ maintained its intensity (20 %), being the base peak the one at 602.0 associated to [**1C₃**-2Br]²⁺. As expected, the peak at 336.5 associated to unreacted imidazole [**C**+H]⁺ considerably decreased (18%).

Moreover, when the **1**:**C** molar ratios were *ca.* 1:2 and 1:3, the ESI-MS in positive ion mode after 48 h displayed the most intense peaks for the **1C₃** clusters [**1C₃**-3Br+2**C**]³⁺ and [**1C₃**-3Br+**C**]³⁺, being the abundance of peaks from mono and bisimidazolium salts lower (ESI, Figure S4, Table S1). The ESI-MS in positive ion mode after 697 h for the 1:3 molar ratio was simplified with the two most important peaks corresponding to [**1C₃**-3Br]³⁺ and [**1C₃**-2Br]²⁺ species (ESI, Figure S4).
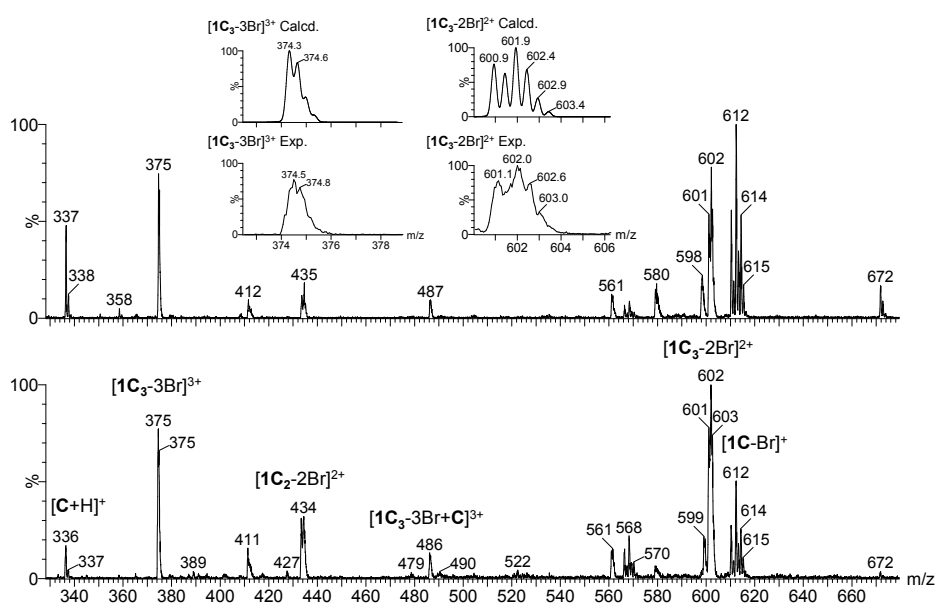

Figure 5 ESI-MS in positive ion mode obtained from an equimolar reaction mixture between tris(bromomethyl)benzene **1** and imidazole **C** after 48 h (top) and 697 h (bottom) of reaction. The initial concentration of both reactants was 13.8 mM. All the assigned peaks provided the correct isotopic pattern. The insets show the comparison of the calculated and observed isotopic patterns for the peaks at 375 and 602.

Some interesting differences were observed when the imidazole **A** was studied in the reaction with 1,3,5-tris(bromomethyl)benzene. Imidazole **A** is identical to **C**, but lacks the amino acid moiety and, accordingly, the supramolecular potential associated to the peptidic bond in pseudopeptides.[15,17] Reaction progress was monitored following the C2-H (imidazolium) and benzylic methylene signals for the tripodal compound **1A₃** initially at 10.38 and 5.54 ppm respectively. For the monosubstituted **1A** and the disubstituted **1A₂** the signals appeared initially at 11.17 and 10.56 ppm respectively (imidazolium C2-H) and 5.68 and 5.63 ppm (benzylic protons). The disappearance of the signals initially at 3.94 and 7.58 ppm for the N-CH₂ and C2-H protons of imidazole **A** and at 4.45 ppm for the benzylic protons of **1** were used to determine the conversion (ESI, Figure S5). These chemical shifts agreed with those for pure **1A₃** or for the model compound **5** (ESI, Figure S6).

Figure 6a shows the kinetic profiles obtained when the reaction was run with an equimolar mixture of imidazole **A** and **1** (13 mM). After 746 h at 25°C, the conversion of the imidazole product was slightly higher than 90 %, but only 17 % of the consumed units were present in the tris(imidazolium) compound **1A₃**, with around 44 % and 28 % being incorporated into **1A₂** and **1A** species respectively. This behaviour clearly departs from the one observed for the pseudopeptidic imidazole **C**, revealing the importance of the amino acid derived fragment in the preferential formation of the tripodal structure **1C₃**, which must be associated to supramolecular interactions involving the pseudopeptidic moiety.

The experiment carried out using a fivefold excess of imidazole **A** over 1,3,5-tris(bromomethyl)benzene **1** provided the expected kinetic profile in the absence of supramolecular assistance (Figure 6b, see ESI Figure S7 for ¹H NMR spectra) with **1A** being the predominant species for the initial period, reaching a maximum yield of *ca.* 9 % at a reaction time of 40 h.

Journal Name

ARTICLE

Afterwards, the yield of **1A** starts to decrease while those for **1A₂** and **1A₃** yields increase, being **1A₂** the predominant species until 170 h of reaction (up to 27 % yield). Finally, after 170 h, the amount of **1A₂** starts also to decrease while the concentration of **1A₃** steadily increases up to reach an essentially quantitative yield for long reaction times.
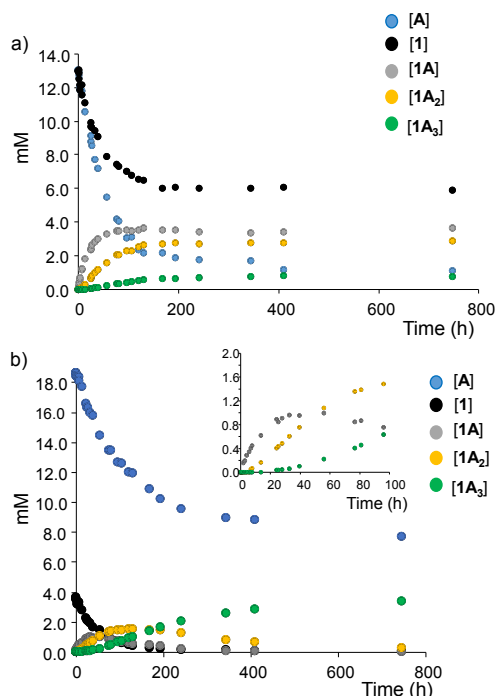

Figure 6 Kinetic profiles for the disappearance of **A** (blue) and **1** (black) and the formation of **1A** (grey), **1A₂** (yellow) and **1A₃** (green) by reaction of **1** and **A** in CDCl₃ at 25ºC following the C2-H protons for **A**, **1A**, **1A₂** and **1A₃** and the benzylic protons for 1. a) using an equimolar ratio of **1** and imidazole **A** (13 mM). b) using a fivefold excess of **A** (18.6 mM) over **1** (3.6 mM).
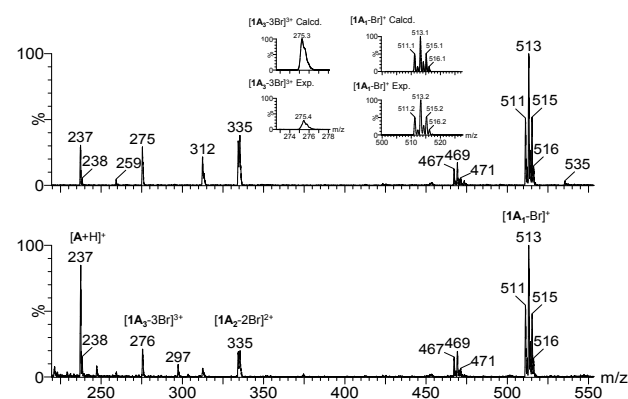

Figure 7 ESI-MS in positive ion mode obtained from an equimolar reaction mixture between tris(bromomethyl)benzene **1** and imidazole **A** after 48 h (bottom) and 747 h (top) of reaction in CDCl₃. The initial concentration of both reactants was 13 mM. All the assigned peaks provided the correct isotopic pattern. The insets show the comparison of the calculated and observed isotopic patterns for the peaks at 275 and 513.

For the equimolar ratio of reagents and a reaction time of 48 h, the ESI-MS in positive ion mode showed the peaks corresponding to the [**1A**-Br]⁺ (513.2, 100 %), [**1A₂**-2Br]²⁺ (335.4, 20 %) and [**1A₃**-3Br]³⁺ (275.4, 20 %) species (Figure 7). At higher reaction times (747 h), the peak at 237.4 associated

to [**A**+H]⁺ decreases (from 80 % to 30 %), the peaks at 335.4 and 275.4 m/z increase (40% and 28% respectively) and the peak at 513.2 m/z associated to [**1A**-Br]⁺ continue being the base peak (100%). When the reaction was run using an excess of **A** (3.9 mM in **1** and 19.9 mM in **A**) the peak for the unreacted imidazole was predominant at 48 h, while the one corresponding to [**1A₃**-3Br]³⁺ (275.4) became the base peak at longer reaction times (ESI, Figure S8, see also Table S2).

The presence of a long aliphatic tail is also an important structural feature of imidazole **C**. Thus, the reaction between **1** and imidazole **D** having a methyl group instead of the dodecyl fragment was also studied by ¹H NMR and ESI-MS to obtain information on its role on the overall process (ESI, Figures S9 and S10). In this case, no significant differences were observed with respect to the use of imidazole **C**, revealing that the aliphatic chain does not play an important role for the observed preference towards the formation of **1C₃** or **1D₃**. Attempts to analyse the reaction of **1** with imidazole **B** lacking both the amino acid derived fragment and the long tail were unsuccessful for the low solubility of the intermediates in CDCl₃. Finally, the effect of changing the tris(halomethyl)arene was also studied. For the process involving imidazole **C** (14.8 mM) and 1,3,5-tris(bromomethyl)-2,4,6-trimethylbenzene **2** (15.6 mM), the conversion was monitored by following the ¹H NMR signals for the C2-H of the imidazole ring and the proton at the stereogenic carbon (initially at 7.81 and 4.24 ppm) in **C** along with the signal initially at 4.58 ppm for the benzylic protons of **2**. The signals for the C2-H imidazolium proton of **2C**, **2C₃** and **2C₂**, initially at 9.93, 9.80 and 9.40 ppm, were used to follow the formation of the different imidazolium species (ESI, Figure S11). The reaction was significantly faster than when using **1**, but again the formation of the tripodal compound **2C₃** was much favoured over that of **2C₂** and **2C**. In this case, **2C₃** became the major species present in the reaction mixture after 0.5 h (ESI, Figure 12a). ESI-MS in positive ion mode also confirmed these data, with the peaks associated to the tripodal species [**2C₃**-3Br]³⁺ and [**2C₃**-2Br]²⁺ being the more intense even at short reaction times (100% and 62% respectively, ESI, Figure S13a). Similar results were obtained for other **2**:**C** ratios (ESI, Figure S12c-d and S13c-d).

On the other hand, when the imidazole **A** (15.7 mM) and **2** (13.8 mM) were used as starting materials, the reaction was again faster than with **1** but the formation of the monosubstituted and disubstituted imidazolium products **2A** and **2A₂** was favoured at all times over the formation of the tripodal compound. When a *ca.* 1:3 molar ratio (**2**:**A**) was used, **2A** and **2A₂** were the predominant imidazolium species up to 11 h of reaction and, later on, the concentration of these species decreased with the tripodal compound **2A₃** becoming predominant (ESI, Figure S14). The formation of the different species was also confirmed by ESI-MS (ESI, Figure S15). Thus, the preferential formation of tripodal species is associated to the presence of the amide group in **C** and **D**.

Some anions, and particularly bromide, are able to act as efficient catalysts in macrocyclization reactions involving S_N2 reactions and other processes of pseudopeptidic molecules.[21] The bromide anion can participate templating a proper

ARTICLE

Journal Name

preorganization of the open chain precursor but also reducing the energy of the transition state through supramolecular interactions. Besides, the increase in the ionic strength of the medium has been reported to slightly increase the reaction rate in the synthesis of some dicationic imidazoliophanes through S_N2 reactions.[13] When the reaction was carried out in the presence of NEt_4Br (9 mM) employing imidazole **C** (16.6 mM) and **1** (7.6 mM) the results obtained revealed that the main effect of the presence of bromide anion was a decrease in the overall conversion rate and in the formation of **1C_3**, although the tripodal compound was still the more abundant species (ESI, Figure S16).

Determination of kinetic constants. From the former experimental kinetic curves, a detailed kinetic analysis was carried out to determine the main kinetic parameters for each specific reaction. The fitting of the experimental data to a model considering a second order reaction for each step was carried out by means of the Levenberg–Marquardt nonlinear least-squares algorithm,[22] using the R and the RStudio software.[23-25] Moreover, the Eyring equation, $k = (k_BT/h)$ $\exp(-\Delta G\ddagger/RT)$,[26] was employed to calculate the Gibbs free energy barrier. Table 1 summarizes the kinetic constants obtained following this approach. Calculated kinetic curves obtained from data in Table 1 show a good agreement with the experimental ones (ESI, Figure S17). Some deviations are observed for very long reaction times that can be associated to

the difficulty in determining with enough accuracy the experimental values by ^{1}H NMR for some of the species at these times and by the potential interference of the formation of unproductive supramolecular complexes between the tripodal species and the starting imidazole (e.g. **C·1C_3**).

Data in Table 1 show that kinetic constants obtained for 1,3,5-tris(bromomethyl)-2,4,6-trimethylbenzene **2** are significantly higher than those for 1,3,5-tris(bromomethyl)benzene **1**. When the pseudopeptidic imidazole **C** is used, k_1 is always smaller than k_2 and k_3, while k_3 is always the smaller constant when imidazole **A** is used, highlighting the role of the amide moiety in the supramolecular assistance for the preferential formation of polytopic imidazolium systems. When analysing the absolute values for the constants, it is important to bear in mind that the concentration of the bromomethyl species has been used directly for the calculations. However, compounds **1** or **2** contain three reactive sites, the monotopic species like **1C** contain two reactive sites and the ditopic species like **1C_2** contain just one reactive site. Thus, a statistical correction provides the corresponding microconstants describing the intrinsic reactivity of the respective bromomethyl groups. This reveals that the intrinsic constants for the formation of **1C_2** and **1C_3** are of the same order and both one order of magnitude higher than that for the formation of **1C**. The intrinsic constant for the formation of **2C_3** is almost two orders of magnitude higher than the one for the formation of **2C**.

Table 1 Kinetic parameters obtained for the different reactions studied in the synthesis of tris(imidazolium) compounds[a,b]

Tripodal final compound	k_1 (M^{-1} h^{-1})	k_2 (M^{-1} h^{-1})	k_3 (M^{-1} h^{-1})	$\Delta G_1\ddagger$ (kcal/mol)	$\Delta G_2\ddagger$ (kcal/mol)	$\Delta G_3\ddagger$ (kcal/mol)
	Macroscopic kinetic constants[b]					
1C_3	0.46 ± 0.01	10.33 ± 1.04	4.43 ± 0.25	17.98 ± 0.01	16.13 ± 0.06	16.63 ± 0.03
1A_3	0.99 ± 0.01	1.75 ± 0.04	0.72 ± 0.04	17.53 ± 0.01	17.18 ± 0.02	17.71± 0.03
2C_3	9.36 ± 0.22	245.49 ±37.81	379.35 ±98.65	16.19 ± 0.01	14.24 ± 0.09	13.99 ± 0.14
2A_3	11.81 ± 0.35	28.96 ± 1.65	9.04 ± 0.74	16.05 ± 0.02	15.51 ± 0.03	16.21 ± 0.05
	Intrinsic kinetic constants					
1C_3	0.15	5.16	4.43			
1A_3	0.33	0.87	0.72			
2C_3	3.12	122.74	379.35			
2A_3	3.94	14.48	9.04			

[a] All the experimental data, obtained using the different studied ratios between substrates, were used for the fitting. [b] k_1, k_2 and k_3 correspond to the formation of the monotopic, ditopic and tripodal compounds respectively.

Interaction studies. ^{1}H NMR studies revealed significant chemical shift variations for the signals of the C*H, NH and C2-H protons in the starting imidazoles **C** and **D** during the course of the reaction (Figure 2, see also ESI, Figure S9c). This suggests the existence of strong supramolecular interactions between the corresponding imidazole and the imidazolium species formed. This was corroborated by the ESI-MS of the reaction crudes with the observation of some clusters involving imidazolium species and the starting imidazole (Figure 5 and ESI, Figure S4). This should be in good agreement with the initial hypothesis regarding the formation of supramolecular complexes between **C** and **1C** or **1C_2** that could favour the formation of **1C_2** and **1C_3**, justifying the predominant formation of tripodal species even when using a

defect of **C**. To analyse this in more detail, imidazole **C** (15 mM) was titrated with the tripodal imidazolium salt **1C_3**, or the analogous mono- and bis-imidazolium model compounds **3** and **4** using CDCl_3 as solvent and the results followed by ^{1}H NMR (Figure 8 and ESI, Figure S18). The addition of increasing quantities of the imidazolium salts produced downfield shifts of the C2-H, amide NH and C*H proton signals of imidazole **C**, along with an upfield shift of the signal for the amide NH protons of the imidazolium salts. This agrees well with the presence of supramolecular imidazole-imidazolium species stabilized through hydrogen bonds involving the anion as the hydrogen bond acceptor and the amide N-H and the acidic hydrogen atoms of the imidazole / imidazolium ring as hydrogen bond donors. The key role played by the amide

Journal Name

ARTICLE

groups and their relevance for the preferential formation of tripodal species is highlighted by the lack of any significant association when imidazole **A**, for which no preferential formation of **1A₃** is observed, was used instead of **C**.
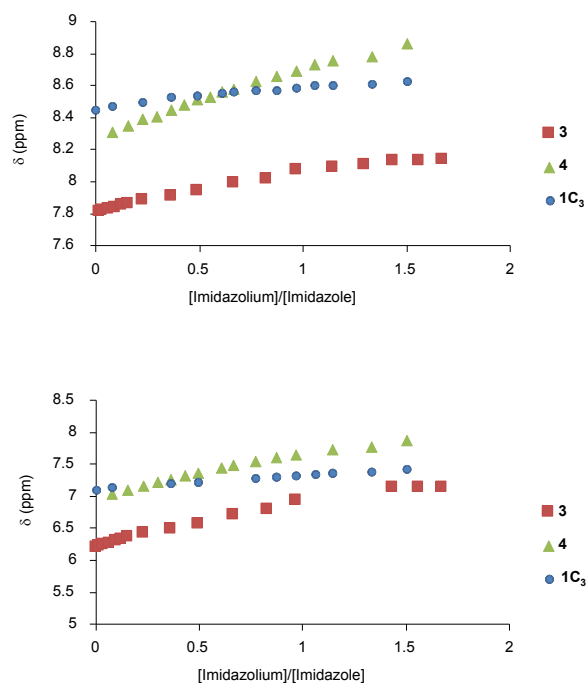

Figure 8 ^{1}H NMR titration curves (500 MHz, CDCl₃) following the imidazole C2-H (top) and the amide N-H (bottom) signals of **C** (15 mM) in the presence of increasing amounts of the monoimidazolium derivative (**3**, red squares), the bisimidazolium model compound (**4**, green triangles) or the tripodal derivative **1C₃** (blue circles).

Titration curves also suggest that the interaction of **C** is stronger with the mono- and bisimidazolium compounds than with **1C₃**. This is of interest as the preferential interaction of **C** with **1C** and **1C₂** can also contribute to promote the preferential formation of **1C₃** in excellent yields even using a limited amount of **C**, avoiding the formation of significant amounts of **C·1C₃**, and can be assigned to the presence of a strong intramolecular hydrogen bonding network in **1C₃**.

In this regard, it must be noted that NMR data suggest the presence of a rigid conformation in **1C₃** with a strong non-equivalence of the two hydrogen atoms of the benzylic groups. Again the amide group is essential for this behaviour as the NMR data for **1A₃** are in agreement with less rigid conformations for this species (ESI, Figure S19). Rather surprisingly, a decrease in rigidity is observed for **2C₃**, as compared with **1C₃**, in spite of the presence of additional methyl groups in the aromatic fragment, which usually is accompanied by loss of conformational freedom in related systems.[15a] This is indicative of a stronger intramolecular hydrogen bonding network in **1C₃** as confirmed by the higher chemical shifts detected for the acidic hydrogen atoms in **1C₃** (9.96 ppm for C2-H in **1C₃** *vs*. 9.55 ppm for **2C₃**). Moreover, ROESY experiments and theoretical studies also supported a rigid arrangement of the three chains in **1C₃** with the C2-H being close to one of the benzylic protons but not to the other

(ESI, Figure S20) and the modelling showing a higher number of H-bonds linking the bromide anions and the imidazolium groups in **1C₃** (ESI, Figure S21).

The role of the bromide anion in the formation of those supramolecular imidazole / imidazolium complexes also explains the observed reduction in reaction rates when using an excess of this anion. Thus, the addition of increasing quantities of bromide anion produced a downfield shift of the signals of the amide NH proton, the imidazole C2-H and the C*H for **C** while no significant changes were observed in the case of **1C₃** (ESI, Figure S22). This supramolecular association between bromide and **C** would make less favourable the formation of the supramolecular complex of this starting material with the initially formed imidazolium species that promote a more rapid reaction. In the presence of excess bromide, imidazole / imidazolium clusters were not detected in ESI-MS experiments (ESI, Figure S16).

Such hydrogen bonding interactions are expected to be very sensible to polar protic solvents. Thus, the reaction between 1,3,5-tris(bromomethyl)benzene **1** (9.0 mM) and imidazole **C** (13.3 mM) was also run in CD₃OD. Following the ^{1}H NMR signals for C*H and C2-H of the imidazole **C** a significant decrease in reactivity was observed (*e.g.* at 498 h only 36% conversion of **C** occurred) (ESI, Figure S23a), H/D exchange did not allow a proper monitoring of C2-H signals in imidazolium species, but positive ion mode ESI-MS experiments after long reaction times (679 h, ESI, Figure S23b) revealed that ditopic and tritopic imidazolium compounds were very minor species, the mono imizadolium compound being the major formed species. This again confirms the key role of the supramolecular interactions involving hydrogen bonding between imidazolium intermediates and starting imidazoles.

Self-Sorting and Competitive Studies. Considering the observed differences between the pseudopeptidic imidazole **C** and imidazole **A** lacking the amino acid derived fragment, additional experiments were carried out to analyse the potential self-sorting when using 1,3,5-tris(bromomethyl) benzene **1** and an excess of an equimolar mixture of imidazoles **A** (13.7 mM) and **C** (13.9 mM) (2.5 equiv. each).[27] Figure 9 shows the ESI-MS in positive ion mode obtained after 480 h of reaction. Although a full self-sorting is not observed the spectrum reveals the preferential incorporation of imidazole **C** into the polytopic imidazolium species. The unreacted imidazole **A** provides the base peak (237, [**A**+H]⁺), while the peak at 336.4 corresponding to [**C**+H]⁺ is very small (<5%). Mixed tripodal species [**1AC**-3Br]³⁺ (m/z: 341.6, 23%) and [**1AC₂**-2Br]²⁺ (552.4, 10%) are more important than those containing two units from **A** like [**1A₂C**-3Br]³⁺ (308.5, 10%). A relatively minor peak is also observed for the homotripodal species [**1C₃**-2Br]²⁺ at 602.1. The ^{1}H NMR spectra also showed a preferential consumption of imidazole **C** (**C**/**A** molar ratio became 0.59 after 184 h) (ESI, Figure S24).
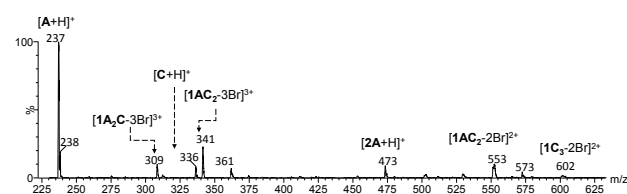
ARTICLE

Journal Name

Figure 9 ESI-MS in positive ion mode for the reaction between **C** (13.9 mM) and **A** (13.7 mM) with **1** (5.5 mM) after 480 h of reaction in CDCl$_3$.

To assess the effect of the length of the aliphatic chain, additional competitive studies were run using a defect of 1,3,5-tris(bromomethyl)benzene **1** and an equimolar mixture of **C** and **D** (3 equiv.). After 120 h of reaction, ESI-MS experiments showed the presence of homo- and heterotritopic species, but with a slight preference for the incorporation of imidazole **D** (ESI, Figure S25 and Table S3). This confirms that, in opposition to the amide fragment, the long aliphatic tail does not participate in the recognition process favouring the formation of the tripodal species. As a matter of fact, the presence of smaller aliphatic fragments seems to facilitate better this process.

Finally, competitive studies were run mixing 1,3,5-tris(bromomethyl)benzene **1** (5 mM) and imidazoles **C** (3 equiv.), **D** (3 equiv.) and **A** (3 equiv.) (ESI, Figure S26). In this case, after 120h, species containing the imidazole building block **D** seems to be favoured, with the most important species detected by ESI-MS in positive ion mode corresponding to [**1D$_3$**-3Br]$^{3+}$ (220, 23%), [**1CD$_2$**-3Br]$^{3+}$ (272, 25%), [**1D$_3$**-2Br]$^{2+}$ (371, 3%) and [**1CD$_2$**-2Br]$^{2+}$ (448, 3%).

Computational studies. In order to get additional insights on the mechanisms involved, a computational study was carried out using Gaussian 16[28] by means of the commonly used DFT functional (B3LYP)[29] using the 6-311+G(d,p) basis set.[30] In order to save computational time, imidazoles **B** and **D** lacking the long dodecyl aliphatic tail were selected as model compounds. This is reasonable taking into account that the change from dodecyl to methyl experimentally plays a minor role in the process. The evaluation of **B** and **D** still allows comparing the effect of the amide group.
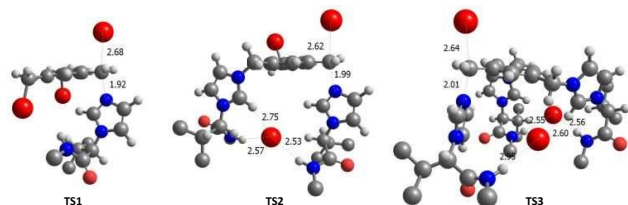

Figure 10 Structures of the calculated transition states obtained for the synthesis of **1D$_3$**.

For the pseudopeptidic compound **D**, the DFT study showed that formation of the monotopic derivative **1D** presents a TS with a higher activation barrier than the one for the formation of the ditopic derivative **1D$_2$**, being this higher than that for the formation of the trisubstituted compound **1D$_3$**. The computed activation free enthalpies (ΔH$^{\ddagger}_{calc}$) were found to be 23.7, 13.5 and 11.1 kcal/mol for **1D**, **1D$_2$** and **1D$_3$**, respectively (ESI, Table

S4). For the imidazole **B**, the DFT study showed that the formation of the monotopic compound **1B** occurs through a TS with a higher activation energy that the one required for the formation of **1B$_2$**; but this last barrier, however, was slightly lower than the one present in the formation of the tripodal derivative **1B$_3$**. The computed activation free enthalpies (ΔH$^{\ddagger}_{calc}$) were in this case 27.0, 23.1 and 24.2 kcal mol^{-1} for **1B**, **1B$_2$** and **1B$_3$**, respectively (ESI, Table S4). When comparing the reaction of imidazole **D** with trisbromomethyl derivatives **1** and **2**, the computed activation barriers for the formation of species derived from **2** were always slightly lower that the ones computed for species derived from **1**. Thus, the methyl substitution on the central aromatic ring accelerates the S$_N$2 reaction as observed experimentally (ESI, Table S4). All the reactions were exergonic with free reaction energy values ranging from -5 to -15 kcal mol^{-1}.

Figure 10 shows the three consecutive transition states calculated for the reaction between **1** and **D**. As can be observed for [TS2]$^{\ne}$ and [TS3]$^{\ne}$, both TSs display intramolecular hydrogen bonds linking the imidazolium and the imidazole fragments involved in the reaction through a bromide anion. In both cases the hydrogen atom at the C2 position of the imidazolium ring participates in the hydrogen bond network, highlighting the supramolecular potential of imidazolium subunits. For [TS2]$^{\ne}$ the imidazolium fragment displays two hydrogen bonds to the bromide involving the amide N-H and the C2-H of the imidazolium ring. The smaller distance calculated for NH···Br$^-$ suggests that this hydrogen bond is stronger than the one with the C2-H as should correspond with its higher acidity. For [TS3]$^{\ne}$ the two imidazolium subunits are hydrogen bonded to one bromide anion. One of them participates with the amide N-H and the C2-H moieties, while the second one only participates with the amide N-H fragment. Thus, the C2-H of this imidazolium group is hydrogen bonded with a second bromide displaying a hydrogen bond with the amide NH of the reacting imidazole. Interestingly, a strong hydrogen bonding of the imidazole units, significantly favouring the formation of the polytopic derivatives, takes place when the amide group is present. Thus, computational results are in excellent agreement with the experimental ones, and support the presence of supramolecular interactions, even at the TS level, of the formed imidazolium groups with the imidazole nucleophiles, particularly relevant for pseudopeptidic systems.

Conclusions

Supramolecular interactions associated to the presence of the peptidic bond are essential in many natural systems but also in pseudopeptidic receptors, and the results presented here show that they are also able to strongly assist the synthesis of polytopic pseudopeptidic imidazolium compounds. The experimental data presented, in good agreement with computational calculations, reveal that in the considered trisimidazolium compounds the introduction of the first imidazolium fragments facilitates the second functionalization by establishing supramolecular interactions with the imidazole

Journal Name

ARTICLE

acting as the nucleophilic reagent. Once the ditopic system is formed, similar supramolecular interactions favour the formation of the tripodal imidazolium system. According to computational calculations, such supramolecular interactions are also present at the corresponding TSs ([TS2]$^{\neq}$ and [TS3]$^{\neq}$). The imidazole/imidazolium groups considered contain three different structural elements of interest for supramolecular interactions: the imidazole/imidazolium group itself, the amide group associated to the amino acid involved, and a long aliphatic tail (dodecyl group). However, the study of similar processes involving other imidazole derivatives lacking either the amide group or the long aliphatic tail has demonstrated that the combination of the imidazole/imidazolium fragments containing an amide group is playing the key role in those supramolecular interactions, while the length of the aliphatic tail does not provide a significant contribution. The importance of this supramolecular assistance is highlighted by the fact that in the case of pseudopeptidic imidazole reagents, the tripodal imidazolium compound is always obtained as the very major product even when a defect of imidazole (e.g. 1/3 of the stoichiometric amount) is used for the reaction. This behaviour is reminiscent of the one found in autocatalytic and self-replicating systems.

Experimental

General: All reagents were purchased from commercial suppliers and used as received. The NMR spectroscopic experiments were carried out at the field reported, at 25 ºC and using trimethylsilane as the internal standard. Microwave reactions were carried out using a Discover System Model 908010 from CEM Corporation using custom-made high purity quarts vials (capacity 10 mL). ESI-MS experiments were recorded on a Q-TOF Premier mass spectrometer with an orthogonal Z-spray electrospray interface (Micromass, Manchester, UK) by electrospray in positive or negative mode.

Synthesis of 1A₃: Compound **A** (0.308 g, 1.27 mmol, 3.3 equiv.) and 1,3,5-tris(bromomethyl)benzene (0.141 g, 0.39 mmol, 1 equiv.) were dissolved in acetonitrile (3 mL) in a microwave tube and heated in a microwave instrument at 150 ºC (120 W) for 1 h. The precipitate obtained was filtered, washed with cold ethyl acetate and vacuum dried. The product was a beige solid (0.38 g, 93%). M.p. (DSC): 178.2 ºC. [α] $_D^{25}$ = -2.51 (c = 0.021, CH₃OH). IR (ATR): 3419, 3083, 2919, 2850, 1553, 1467 cm⁻¹. ¹H NMR (300 MHz, CDCl₃) δ= 10.44 (s, 3H), 8.65 (s, 3H), 8.63 (s, 3H), 7.06 (s, 3H), 5.54 (s, 6H), 4.22 (q, J = 7.6, 6.2 Hz, 6H), 1.25 (s, 6H), 1.40-1.17 (m, 54H), 0.95 − 0.79 (m, 9H). ¹³C NMR (101 MHz, CDCl₃): δ= 136.5, 135.5, 132.0, 124.5, 121.2, 52.1, 50.3, 31.9, 30.1, 29.6, 29.6, 29.5, 29.4, 29.3, 29.0, 26.3, 22.6, 14.1 ppm. MS (ESI⁺): m/z (%) = 275 (100) [C₅₄H₉₃N₆]³⁺. Calculated for C₅₄H₉₃N₆Br₃·3.5 H₂O: C 57.4, H 8.9, N 7.4; found C 57.4, H 8.4, N 7.2.

Synthesis of 2A₃: Compound **A** (0.100 g, 0.42 mmol, 3.3 equiv.) and 1,3,5-tris(bromomethyl)-2,4,6-trimethylbenzene (0.057 g, 0.13 mmol, 1 equiv.) were dissolved in chloroform (5 mL) and stirred in a round bottom flask (25 mL) for 5 days at rt. The reaction gave a yellow solid product (0.13 g, 94%). M.p. (DSC):

297.5 ºC. [α] $_D^{25}$ = -0.45 (c = 0.021, CH₃OH). IR (ATR): 3432, 3067, 2921, 2852, 1559, 1465 cm⁻¹. ¹H NMR (400 MHz, CDCl₃) δ= 10.00 (s, 3H), 8.43 (s, 3H), 7.28 (s, 3H), 5.80 (s, 6H), 4.31 (t, J = 7.4 Hz, 6H), 2.34 (s, 9H), 2.20 (s, 6H), 1.41-1.13 (m, 54H), 0.87 (t, J= 6.8 Hz, 9H). ¹³C NMR (101 MHz, CDCl₃): δ= 142.0, 135.5, 136.0, 129.0, 124.1, 121.7, 50.0, 49.3, 31.9, 30.5, 29.6, 29.6, 29.4, 29.3, 29.1, 26.3, 22.7, 17.7 14.1 ppm. MS (ESI⁺): m/z (%) = 290 (100) [C₅₇H₉₉N₆]³⁺, 474 (31) [C₅₇H₉₉N₆Br]²⁺. Calculated for C₅₇H₉₉N₆Br₃·4.5 H₂O: C 57.6, H 9.2, N 7.1; found C 57.7, H 8.6, N 6.6.

Synthesis of 1C₃: Compound **C** (0.299 g, 0.89 mmol, 3.3 equiv.) and 1,3,5-tris(bromomethyl)benzene (0.079 g, 0.22 mmol, 1 equiv.) were dissolved in acetonitrile (2.23 mL) in a microwave tube and heated in a microwave instrument at 150 ºC (120 W) for 1 h. The solvent was evaporated, and the residue washed with cold ethyl acetate and vacuum dried. The product was a beige solid (0.33 g, 97%). M.p. (DSC): 184.8 ºC. [α] $_D^{25}$ = 13.77 (c = 0.021, CH₃OH). IR (ATR): 3227, 3063, 2921, 2952, 1679 cm⁻¹. ¹H NMR (400 MHz, CDCl₃) δ= 9.97 (s, 3H), 8.37 (d, J = 19.4 Hz, 6H), 8.10 (s, 3H), 7.39 (s, 3H), 5.50 (dd, J = 185.7, 14.1 Hz, 6H), 5.02 (d, J = 10.7 Hz, 3H), 3.30 (m, 3H), 2.91 − 2.29 (dm, 6H), 1.59 − 1.37 (m, 6H), 1.35 − 1.08 (m, 54H), 1.01 (dd, J = 12.0 Hz, 9H), 0.81 (t, J = 6.9 Hz, 9H), 0.70 (dd, J = 6.6 Hz, 9H). ¹³C NMR (126 MHz, CDCl₃): δ= 163.6, 133.3, 132.8, 129.1, 121.7, 116.9, 65.9, 49.6, 37.3, 29.3, 28.4, 27.0, 26.7, 26.5, 24.4, 20.1, 16.2, 15.7, 11.5 ppm. MS (ESI⁺): m/z (%) = 374.5 (100) [C₆₉H₁₂₀N₉O₃]³⁺, 602.0 (45) [C₆₉H₁₂₀N₉O₃Br]²⁺.Calculated for C₆₉H₁₂₀N₉O₃Br₃·H₂O: C 60.0, H 8.9, N 9.2; found C 59.8, H 8.4, N 9.5.

Synthesis of 2C₃: Compound **C** (0.100 g, 0.30 mmol, 3.3 equiv.) and 1,3,5-tris(bromomethyl)-2,4,6-trimethylbenzene (0.040 g, 0.10 mmol, 1 equiv.) were dissolved in dichloromethane (2.23 mL) in a microwave tube and heated in a microwave instrument at 150 ºC (120 W) for 1 h. The solvent was evaporated, and the residue washed with dimethyl ether and vacuum dried. The product was a beige solid (0.099 g, 94%). M.p. (DSC): 153.2 ºC. [α] $_D^{25}$ = -45.89 (c = 0.021, CH₃OH). IR (ATR): 3240, 3062, 2923, 2853, 1678 cm⁻¹. ¹H NMR (400 MHz, CDCl₃) δ= 9.60 (s, 3H), 8.08 (s, 3H), 7.94 (s, 3H), 7.73 (d, J=20.6 Hz, 3H), 6.43-5.20 (m, 6H), 5.38 (d, J = 10.2 Hz, 3H), 3.33 (m, 3H), 3.04 (m, 3H), 2.39 (s, 6H), 2.37 (s, 9H), 1.52 (s, 3H), 1.23 (s, 54H), 1.06 (dd, J = 25.2, 6.5 Hz, 9H), 0.87 (t, J = 6.9 Hz, 9H), 0.74 (d, J = 6.1 Hz, 9H). ¹³C NMR (101 MHz, CDCl₃): δ= 166.8, 142.0, 135.7, 129.0, 121.6, 67.6, 49.4, 39.9, 31.9, 29.6, 29.2, 27.0, 22.7, 18.8, 18.3, 17.5, 14.1 ppm. MS (ESI⁺): m/z (%) = 623.0 (100) [C₇₂H₁₂₅N₉O₃Br]²⁺, 388.6 (91) [C₇₂H₁₂₆N₉O₃]³⁺. Calculated for C₇₂H₁₂₆N₉O₃Br₃·H₂O: C 60.8, H 9.1, N 8.9; found C 60.5, H 9.2, N 8.9.

Synthesis of 1D₃: Compound **D** (0.100 g, 0.55 mmol, 3.3 equiv.) and 1,3,5-tris(bromomethyl)benzene (0.068 g, 0.19 mmol, 1 equiv.) were dissolved in chloroform (5 mL) and stirred in a round bottom flask (25 mL) for 5 days at rt. The solvent was evaporated, and the residue washed with dimethyl ether and vacuum dried. The product was a beige solid (0.053 g, 89%). [α] $_D^{25}$ = 38.75 (c = 0.021, CH₃OH). IR (ATR): 3397, 3077, 2967, 1673, 1550 cm⁻¹. ¹H NMR (400 MHz, CDCl₃) δ= 10.01 (s, 3H), 8.43 (s, 3H), 8.41 (s, 3H), 8.19 (s, 3H), 7.48 (s, 3H), 5.57 (dd,

ARTICLE

Journal Name

J=122.3, 14.1 Hz, 6H), 5.08 (d, J=10.8 Hz, 3H), 2.72 (d, J = 4.6 Hz, 9H), 2.40 (m, 3H) 0.92 (dd, J = 110.8, 6.6 Hz, 18H). ^{13}C NMR (101 MHz, CDCl$_3$): δ= 166.9, 135.8, 135.4, 131.8, 124.3, 119.6, 74.5, 68.4, 52.2, 30.8, 26.2, 18.8, 18.3 ppm. MS (ESI$^+$): m/z (%) = 220 (100) [C$_{36}$H$_{54}$N$_9$O$_3$]$^{3+}$. Calculated for C$_{36}$H$_{54}$N$_9$O$_3$Br$_3$: C 62.0, H 8.4, N 18.1; found C 62.1, H 8.3, N 18.0.

Synthesis of 2D$_3$: Compound **D** (0.100 g, 0.55 mmol, 3.3 equiv.) and 1,3,5-tris(bromomethyl)-2,4,6-trimethylbenzene (0.075 g, 0.19 mmol, 1 equiv.) were dissolved in chloroform (5 mL) and stirred in a round bottom flask (25 mL) for 5 days at rt. The solvent was evaporated, and the residue washed with dimethyl ether and vacuum dried. The product was a beige solid (0.133 g, 84%). M.p. (DSC): 362.7 ºC. [α] $_D^{25}$ = 2.62 (c = 0.021, CH$_3$OH). IR (ATR): 3395, 3232, 3073, 2967, 1673, 1546 cm^{-1}. ^{1}H NMR (400 MHz, CDCl$_3$) δ= 9.54 (s, 3H), 8.16 (s, 3H), 7.84 (s, 3H), 7.72 (s, 3H), 5.66 (d, J=19.7 Hz, 6H), 5.26 (d, J=10.1 Hz, 3H), 2.70 (d, J=4.2 Hz, 9H), 2.45 (s, 9H), 2.40 (s, 3H), 0.96 (d, J=6.5 Hz, 9H), 0.68 (d, J=6.5 Hz, 9H). ^{13}C NMR (101 MHz, CDCl$_3$): δ= 167.4, 142.0, 135.7, 129.07, 122.8, 121.7, 67.7, 49.5, 31.4, 26.3, 18.8, 18.3, 17.6 ppm. MS (ESI$^+$): m/z (%) = 234 (100) [C$_{39}$H$_{60}$N$_9$O$_3$]$^{3+}$. Calculated for C$_{39}$H$_{60}$N$_9$O$_3$Br$_3$·8H$_2$O: C 43.1, H 7.1, N 11.6; found C 43.4, H 6.5, N 11.0.

Computational details: The calculations were performed with the Gaussian 16 program using the widely used DFT method based on Becke's GGA exchange functional B3LYP with standard 6-311+G(d,p) basis set. The stationary points were fully characterized by means of harmonic vibrational frequency analysis. For all of the transition structures, the normal mode related to the imaginary frequency corresponds to the nuclear motion along the reaction coordinates under study. Additionally, we carried out intrinsic reaction coordinate calculations (IRC) to verify that the transition structures were connected with reactants and products.

Conflicts of interest

There are no conflicts to declare

Acknowledgements

Notes and references

1   (a) N. S. Hong, D. Petrović, R. Lee, G. Grynova, M. Purg, J. Saunders, P. Bauer, P. D. Carr, C.-Y. Lin, P. D. Mabbitt, W. Zhang, T. Altamore, C. Easton, M. L. Coote, S. C. L. Kamerlin and C. J. Jackson, *Nat. Commun.*, 2018, **9**, 3900; (b) D. Petrovic, V. A. Risso, S. C. L. Kamerlin and J. M. Sanchez-Ruiz, *J. Royal. Soc. Interface,* 2018, **15**, 1742; (c) V. L. Schramm, *Acc. Chem. Res*., 2015, **48**, 1032.
2   (a) T. D. H. Bugg, *Introduction to Enzyme and Coenzyme Chemistry*, 2012, Wiley.

3   G. P. Horsman, S. Bhowmik, S. Y. Seah, P. Kumar, J. T. Bolin, and L. D. Eltis, *J. Biol. Chem.* 2007, **282**, 19894.
4   (a) D. Yang, J. Zhao, X.J. Yang and B. Wu, *Org. Chem. Front.*, 2018, **5**, 662; (b) V. Zanichelli, G. Ragazzon, G. Orlandini, M. Venturi, A. Credi, S. Silvi, A. Arduini and A. Secchi, *Org. Biomol. Chem.*, 2017, **15**, 6753; (c) V. Marti-Centelles, M. D. Pandey, M. I. Burguete and S.V. Luis, *Chem. Rev.*, 2015, **115**, 8736; (d) A. B. Pun, K. J. Gagnon, L. M. Klivansky, S. J. Teat, Z. T. Li and Y. Liu, *Org. Chem. Front.*, 2014, **1**, 167.
5   (a) V. Martí-Centelles, M. I. Burguete and S. V. Luis, *J. Org. Chem.*, 2016, **81**, 2143; (b) V. Martí-Centelles, M. I. Burguete and S. V. Luis, *Chem. Eur. J.,* 2012, **18**, 2409; (c) M. Bru, I. Alfonso, M. Bolte, M. I. Burguete and S. V. Luis, *Chem. Commun.,* 2011, **47**, 283; (d) I. Alfonso, M. Bolte, M. Bru, M. I. Burguete, S. V. Luis and J. Rubio, *J. Am. Chem. Soc.,* 2008, **130**, 6137; (e) I. Alfonso, M. Bolte, M. Bru, M. I. Burguete and S. V. Luis, *Chem. Eur. J.,* 2008, **14**, 8879; (f) M. Bru, I. Alfonso, M. I. Burguete and S. V. Luis, *Tet. Letters,* 2005, **46**, 7781; (g) J. Becerril, M. Bolte, M. I. Burguete, F. Galindo, E. García-España, S. V. Luis and J. F. Miravet, *J. Am. Chem. Soc.,* 2003, **125**, 6677; (h) A. Andrés, M. I. Burguete, E. García-España, S. V. Luis, J. F. Miravet and C. Soriano, *J. Chem. Soc., Perkin 2*, 1993, 749.
6   A. M. Maharramov, K. T. Mahmudov, M. N. Kopylovich, A. J. L. Pombeiro, *Non-covalent Interactions in the Synthesis and Design of New Compounds,* Wiley, 2016.
7   (a) M. Altay, Y. Altay, S. Otto, *Angew. Chem. Int. Ed.* 2018, **57**, 10564; (b) T. Kosikova and D. Philp, *Chem. Soc. Rev.* 2017, **46**, 7274; (c) H. Duim and S. Otto, *Beilstein J. Org. Chem.* 2017, **13**, 1189; (d) G. Clixby and L. Twyman*, Org. Biomol. Chem.* 2016, **14**, 4170; (e) T. A. Plöger and G. von Kiedrowski, *Org. Biomol. Chem.*, 2014, **12**, 6908; (f) A. J. Bissette and S. P. Fletcher, *Angew. Chem. Int. Ed.*, 2013, **52**, 12800; (g) V. Rotello, J. I. Hong and J. Rebek, *J. Am. Chem. Soc.*, 1991, **113**, 9422.
8   (a) S. Kamioka, D. Ajami and J. Rebek, *PNAS*, 2010, **107**, 541; (b) A. Vidonne and D. Philp. *Eur. J. Org. Chem.* 2009, 593; (c) T. Tjivikua, P. Ballester and J. Rebek, *J. Am. Chem. Soc.*, 1990, **112**, 1249.
9   (a) E. A. Wintner, M. M. Conn and J. Rebek, *J. Am. Chem. Soc.*, 1994, **116**, 8877; (b) M. M. Conn, E. A. Wintner and J. Rebek, *J. Am. Chem. Soc.,* 1994, **116**, 8823; (c) M. M. Conn, E. A. Wintner and J. Rebek, *Angew. Chem. Int. Ed.*, 1994, **33**, 1577; (d) Q. Feng, T. K. Park and J. Rebek, *Science*, 1992, **256**, 1179; (e) J. S. Nowick, Q. Feng, T. Tjivikua, P. Ballester and J. Rebek, *J. Am. Chem. Soc.*, 1991, **113**, 8831.
10 D. H. Lee, K. Severin, M. R. Ghadiri, *Curr. Opin. Chem. Biol.*, 1997, **1**, 491.
11 (a) S. Kamioka, D. Ajami and J. Rebek. Jr., *Chem. Commun.*, 2009, 7324; (b) J. Chen, S. Korner, S. L. Craig, D. M. Rudkevich and J. Rebek, *Nature*, 2002, **415**, 385.
12 (a) Y. D. Yang, J. L. Sessler and H. Y. Gong, *Chem. Commun.*, 2017, **53**, 9684; (b) Z. Xu, S. K. Kim and J. Yoon*, Chem. Soc. Rev.*, 2010, **39**, 1457.
13 (a) E. Alcalde, N. Mesquida, M. Vilaseca, C. Alvarez-Rúa and S. García-Granda, *Supramol. Chem.,* 2007, **19**, 501; (b) S. Ramos, E. Alcalde, G. Doddi and P. Mencarelli, *J. Org. Chem.*, 2002, **67**, 8463; (c) E. Alcalde, S. Ramos and L. Perez-García, *Org. Lett.,* 1999, **1**, 1035.
14 (a) R. Rondla, *Inorganica Chimica Acta,* 2018, **477**, 183; (b) S. Ruiz-Botella, P. Vidossich, G. Ujaque, E. Peris and P. D. Beer, *RSC Adv.*, 2017, **7**, 11253; (c) F. D'Anna and R. Notto, *Eur. J. Org. Chem*., 2014, 4201; (d) N. Alhashimy, D. J. Brougham, J. Howarth, A. Farrell, B. Quilty and K. Nolan, *Tetrahedron Letters,* 2007, 48, 125; (e) H. Ihm, S. Yun, H. Gon Kim, J. K. Kim, and K, S. Kim, *Org. Lett.,* 2002, **4**, 2897.
15 (a) L. Gonzalez, J. Escorihuela, B. Altava, M.I. Burguete and S.V. Luis, *Org. Biomol. Chem.* 2015, **13**, 5450; (b) L. Gonzalez,

ARTICLE

B. Altava, M.I. Burguete, J. Escorihuela, E. Hernando, S. V. Luis, R. Quesada and C. Vicent, *RSC Adv.*, 2015, **5**, 34415.

16 (a) M. Savastano c. Bazzicalupi, C. Garcia-Gallarin, M.D.L. de la Torre, A. Bianchi and M. Melguizo, *Org. Chem. Front.*, 2019, **6**, 75; (b) A. Shokri, S. H. M. Deng, X. B. Wang and S. R. Kass, *Org. Chem. Front.*, 2014, **1**, 54; (c) H. J. Schneider and A. K. Yatsimirsky, *Chem. Soc. Rev.*, 2008, **37**, 263; (d) V. Amendola and L. Fabbrizzi, *Acc. Chem. Res.*, 2006, **39**, 343; (e) K. Bowman-James, *Acc. Chem. Res.*, 2005, **38**, 671; (f) A. Bianchi, K. Bowman-James and E. Garcia-España, *The Supramolecular Chemistry of Anions*, Wiley-VCH, Weinheim, 1997.

17 (a) S. V. Luis and I. Alfonso, *Acc. Chem. Res.*, 2014, **47**, 112; (b) L. Kaufmann, N. L. Trautsen, A. Springer, H. V. Schroder, T. Makela, K. Rissanen and C. A. Schalley, *Org. Chem. Front.s*, 2014, **1**, 521.

18 (a) L. Y. Sun, N. Sinha, T. Yan, Y. S. Wang, T. T. Y. Tan, L. Yu, Y. F. Han, and F. E. Hahn, *Angew. Chem. Int. Ed.*, 2018, **57**, 5161; (b) R. Zhong, Y. N. Wang, X. Q. Guo, X. F. Hou, *J. Organomet. Chem*., 2011, **696**, 1703; (c) C. E. Willans, K. M. Anderson, P. C. Junk, L. J. Barbour and J. W. Steed, *Chem. Commun.*, 2007, 3634; (d) A. Metzger and E. V. Anslyn, *Angew. Chem. Int. Ed.,* 1998, **37**, 649.

19 (a) E. Faggi, R. Porcar, M. Bolte, S. V. Luis, E. García-Verdugo and I. Alfonso, *J. Org. Chem*., 2014, **79**, 9141; (b) I. Martí, J. Rubio, M. Bolte, M. I. Burguete, C. Vicent, R. Quesada, I. Alfonso and S. V. Luis, *Chem. Eur. J.,* 2012, **18**, 16728; (c) I. Martí, M. Bolte, M. I. Burguete, C. Vicent, I. Alfonso and S. V. Luis, *Chem. Eur. J.*, 2014, **20**, 7458.

20 L. González, B. Altava, M. Bolte, M. I. Burguete, E. García-Verdugo and S. V. Luis, *Eur. J. Org. Chem.,* 2012, 4996.

21 (a) V. Martí-Centelles, M. I. Burguete, C. Cativiela and S. V. Luis, *J. Org. Chem*., 2014, **79**, 559; (b) E. A. Kataev, G.V. Kolesnikov, R. Arnold, H. V. Lavrov, V. N. Khrustalev, *Chem. Eur. J.,* 2013, **19**, 3710; (c) V. Martí-Centelles, M. I. Burguete, F. Galindo, A. M. Izquierdo, D. K. Kumar, A. J. P. White, S. V. Luis and R. J. Vilar, *J. Org. Chem.*, 2012, **77**, 490.

22 T. V. Elzhov, K. M. Mullen, A. N. Spiess and B. Bolker, *minpack.lm: R Interface to the Levenberg-Marquardt Nonlinear LeastSquares Algorithm Found in MINPACK, Plus Support for Bounds (R package version 1.2-0),* 2015. https://CRAN.R-project.org/package= minpack.lm (accessed January 23, 2018).

23 R Core Team. *R: A language and environment for statistical computing*; R Foundation for Statistical Computing: Vienna, Austria, 2015. https://www.R-project.org/ (accessed January 23, 2018).

24 Studio Team. *RStudio: Integrated Development for R, version 0.99.89*2; RStudio, Inc.: Boston, MA, 2015. http://www.rstudio.com/ (accessed January 23, 2018)

25 V. Martí-Centelles, A. L. Lawrence and P. J. Lusby, *J. Am. Chem. Soc.*, 2018, **140**, 2862.

26 (a) K. J. Laidler, M. C. King, *J. Phys. Chem*., 1983, **87**, 2657; (b) G. A. Petersson, *Theor. Chem. Acc*., 2000, **103**, 190.

27 (a) B. Zheng, F. Klautzsch, M. Xue, F. H. Huang and C. A. Schalley, *Org. Chem. Front.*, 2014, **1**, 532; (b) M. Kołodziejski, A. R. Stefankiewicz and J.-M. Lehn, *Chem. Sci.*, 2019, **10**, 1836.

28 Gaussian 16, Revision B.01, M. J. Frisch, G. W. Trucks, H. B. Schlegel, G. E. Scuseria, M. A. Robb, J. R. Cheeseman, G. Scalmani, V. Barone, G. A. Petersson, H. Nakatsuji, X. Li, M. Caricato, A. V. Marenich, J. Bloino, B. G. Janesko, R. Gomperts, B. Mennucci, H. P. Hratchian, J. V. Ortiz, A. F. Izmaylov, J. L. Sonnenberg, D. Williams-Young, F. Ding, F. Lipparini, F. Egidi, J. Goings, B. Peng, A. Petrone, T. Henderson, D. Ranasinghe, V. G. Zakrzewski, J. Gao, N. Rega, G. Zheng, W. Liang, M. Hada, M. Ehara, K. Toyota, R. Fukuda, J. Hasegawa, M. Ishida, T. Nakajima, Y. Honda, O. Kitao, H. Nakai, T. Vreven, K. Throssell, J. A. Montgomery, Jr., J. E. Peralta, F. Ogliaro, M. J. Bearpark, J. J. Heyd, E. N. Brothers, K. N. Kudin, V. N. Staroverov, T. A. Keith, R. Kobayashi, J. Normand, K. Raghavachari, A. P. Rendell, J. C. Burant, S. S. Iyengar, J. Tomasi, M. Cossi, J. M. Millam, M. Klene, C. Adamo, R. Cammi, J. W. Ochterski, R. L. Martin, K. Morokuma, O. Farkas, J. B. Foresman, and D. J. Fox, Gaussian, Inc., Wallingford CT, 2016.

29 (a) A. D. Becke*, J. Chem. Phys*., 1993, **98**, 1372; (b) A. D. Becke, *J. Chem. Phys*., 1993, **98**, 5648; c) C. Lee, W. Yang and R. G. Parr, *Phys. Rev. B: Condens. Matter*, 1988, **37**, 785.

30 A. Höllwarth, M. Bohme, S. Dapprich, A. Ehlers, A. Gobbi, V. Jonas, K. F. Köhler, R. Stegmann, A. Veldkamp and G. Frenking, *Chem. Phys. Lett*., 1993, **208**, 237.